Revista Brasileira de Recursos Hídricos
Brazilian Journal of Water Resources
Versão On-line ISSN 2318-0331
RBRH, Porto Alegre, v. 25, e39, 2020
Scientific/Technical Article

https://doi.org/10.1590/2318-0331.252020200052

Mathematical modeling of the infiltration in a permeable pavement on the field scale

Modelagem matemática da infiltração em um pavimento permeável na escala de campo

Marília Neves Marinho[1], Artur Paiva Coutinho[1], Severino Martins dos Santos Neto[2], Cézar Augusto Casagrande[1], Guilherme Teotônio Leite Santos[1] & Arnaldo Manoel Pereira Carneiro[2]

[1]Universidade Federal de Pernambuco, Caruaru, PE, Brasil
[2]Universidade Federal de Pernambuco, Recife, PE, Brasil

E-mails: marilianmarinho@yahoo.com.br (MNM), arthur.coutinho@yahoo.com.br (APC), martinsdsn@gmail.com (SMSN), cezar.acasa@gmail.com (CAC), guilherme3tls@hotmail.com (GTLS), arnaldo2164@hotmail.com (AMPC)

Received: March 12, 2020 - Revised: June 16, 2020 - Accepted: June 22, 2020

ABSTRACT

Permeable pavement (PP) is an alternative for the management of urban rainwater that allows the reduction of effective precipitation through the infiltration process. In this study was evaluated the infiltration capacity of a PP of hollow concrete blocks in a parking lot of the Federal University of Pernambuco. The hydraulic characterization and the infiltration capacity were analyzed in real scale, using a simple ring infiltrometer of 100 cm in diameter through the Beerkan method. Infiltration tests were carried out at twelve points of the PP. The BEST algorithm was applied in it Best-Intercept and Best-Slope version, to estimate the hydraulic parameters of the van Genutchen and Brooks and Corey equations for the retention and hydraulic conductivity of the PP surface. The values of saturated hydraulic conductivity determined by the BEST Intercept method were higher than those obtained by BEST Slope. The sorptivity values estimated by BEST Slope and Intercept were similar, with BEST Slope values slightly higher. Moderate infiltration variability was observed on the PP surface, as well as within the same type of texture. The Beerkan method proved to be adaptable to measure, in field scale, the three-dimensional infiltration in the PP covering layer.

Keywords: Hollow concrete blocks; Urban drainage; Hydraulic characterization; Beerkan method.

RESUMO

Pavimento permeável é uma alternativa para o manejo das águas pluviais urbanas que permite a redução da precipitação efetiva através do processo de infiltração. O estudo avaliou a capacidade de infiltração de um pavimento permeável (PP) de blocos vazados de concreto no estacionamento da Universidade Federal de Pernambuco. A caracterização hidrodinâmica e a capacidade de infiltração foram analisadas em escala real, utilizando infiltrômetro de anel simples de 100 cm de diâmetro através do método Beerkan. Realizaram-se ensaios de infiltração em doze pontos do PP. Foi aplicado o algoritmo BEST na sua versão Best-Intercept e Best-Slope, para a estimativa dos parâmetros hidrodinâmicos da equação de van Genutchen e Brooks e Corey para as curvas de retenção e de condutividade hidráulica da superfície do pavimento permeável. Os valores da condutividade hidráulica saturada determinados pelo método BEST Intercept foram superiores aos obtidos pelo BEST Slope. Os valores da Sorvidade estimados pelo BEST Slope e Intercept foram semelhantes, sendo os valores do BEST Slope ligeiramente superiores. Observou-se moderada variabilidade da infiltração na superfície do PP, como também dentro do mesmo tipo de textura. O método Beerkan demonstrou ser adaptável para medir, em escala de campo, a infiltração tridimensional na camada de revestimento do pavimento permeável.

Palavras-chave: Blocos vazados de concreto; Drenagem urbana; Caracterização hidráulica; Método Beerkan.

INTRODUCTION

In Brazil, due to the expansion of the built areas, generally spatially disordered, mainly in the large metropolitan regions with high urbanization, it has caused problems for the management of the stormwater runoff. Population growth and waterproofing of surfaces decrease the natural recharge of groundwater and the quality of surface water. According to Hager et al. (2019), traditional urban rainwater infrastructure is becoming increasingly insufficient due to the rapid urbanization process. In addition, the increase in runoff volume makes it urgent to apply Best Management Practices (BMPs) that favor the natural phenomena of infiltration and storage of urban rainwater (Li et al., 2019).

The management of urban rainwater has become a major challenge in coastal cities with a tropical climate. In these cities, the high frequency of rainfall, with great intensity and volume, associated with hydrographic basins with high waterproofing, bring serious problems and social, environmental, patrimonial and economic damages (Tucci, 2007). In particular, the city of Recife, located in the Northeast of Brazil, has an average annual rainfall of 2400 mm, of which 70% occurs in a concentrated manner between the months of March to August, a period with high flood records (Coutinho, 2011). The typical rainfall intensity for a 25-year return period event with 60 min duration in Recife was estimated at 66,46 $mm.h^{-1}$ (Coutinho et al., 2013).

The use of green technologies that value infiltration and storage phenomena has been reported in several Brazilian studies (Agostinho & Poleto, 2012; Souza et al., 2012; Benini, 2015; Maruyama & Franco, 2016; Nunes et al., 2017). The compensatory technical term for urban drainage has been used in Brazil, assuming the equivalent of Best Management Practices (BMPs) in the United States. Among the alternative techniques for the management of urban rainwater, such as infiltration trenches, infiltration ditches and rain gardens, permeable pavements (PP's) have been increasingly used in sidewalks and parking lots to improve rainwater infiltration in urban (Liu et al., 2019). For the popularization of the use of this technology in Brazil, it is essential to prove its effectiveness in reducing rainwater inundations by the precise estimate of the PP's hydraulic parameters.

PP's are formed by a layer of porous covering and a reservoir of stones. In this type of structure, the knowledge of the infiltration capacity of the wear layer is essential to verify its hydrological performance. For this, the performance of infiltration tests in field scale, in the pavement structure, can estimate the hydraulic properties with the water retention curve and the hydraulic conductivity curve, helping in the decision making regarding the maintenance of the device.

In this sense, several studies such as that by Jabur et al. (2015) and Coutinho et al. (2016), has characterized the infiltration of PP's using the methodology provided for in ASTM (American Society for Testing and Materials) C1701 - Standard Test Method for Infiltration Rate of in Place Pervious Concrete (American Society for Testing and Materials, 2009). However, this method does not allow the estimation of the parameters of the water retention curves and the hydraulic conductivity curve of the soil. The parameters of both curves are prerequisites for the evaluation of hydraulic operating scenarios of the PP's through unsaturated numerical modeling, based on the resolution of the Richards (1931) equation.

Different methods can be used to determine the hydraulic parameters. The method must be chosen according to its complexity, robustness and related costs, among the various methods available the Beerkan method has been widely used (Coutinho et al., 2016). The Beerkan method is a semi-physical method that allows the estimation of seven hydraulic parameters, allowing to appreciate the properties of the water retention curve and the hydraulic conductivity curve of the soil (Lassabatère et al., 2006). Coutinho et al., (2016) used the Beerkan method with 7.5 cm diameter infiltrometers for the hydraulic characterization of fifty-two infiltration tests on a permeable pavement in the city of Recife. Obtaining the hydraulic parameters allowed the authors to simulate the water transfer processes on the permeable pavement.

This study aims to the estimation of hydraulic parameters of the PP wear layer using an analytical inverse technique (i.e. BEST) and Beerkan infiltration test., using the BEST algorithm - Beerkan Estimation of Soil Transfer Parameters through Infiltration Experiments in their Best-Slope and Best-Intercept versions.

MATERIAL AND METHOD

Study site and soil charachterization

The study was carried out on a permeable pavement (PP) implanted in the parking lot of the Center for Legal Science (CCJ) of the Federal University of Pernambuco in Recife at coordinates 8°03'31"S and 34°52'57"W (Figure 1). The climate of the study area is hot and humid with an average annual temperature of 25.8 °C (Köppen As').

Rainfall data from APAC (Pernambuco and Water and Climate Agency) for the period between the years 2010 and 2017 indicate annual average rainfall of 2,167.35 mm. June is the month with the highest rainfall, on average 379.7 mm; and November the driest month, with an average of 37.9 mm (Agência Pernambucana de Águas e Clima, 2018). Winter corresponds to the rainy season and lasts from March to August with about 70% of the total annual rainfall (Figure 2).

The PP investigated in this study was built in 2012 (Figure 3), has been in use for 6 years and has not yet undergone any maintenance. It consists in a layer of concrete hollow blocks, seated on a 7 cm thick layer of sand. The blocks are filled with grass and measure 39 cm × 21 cm and thickness of 10 cm. In this structure, it is considered that the global infiltration capacity of the PP depends mainly on the infiltration capacity of the soil that fills the concrete blocks during rain events. The effects of the lower layers on the infiltration of water were neglected. As a main approach, the focus is placed on the hydraulic characterization of the soil elements of the PP during a typical hydrological year in the region. The soil characterization was carried out in the samples taken from the hollow part of the concrete blocks according to the ABNT NBR 7181/2016 (Associação Brasileira de Normas Técnicas, 2016), the granulometric classification by United States Department of Agriculture (1993) and Empresa Brasileira de Pesquisa Agropecuária (1999).

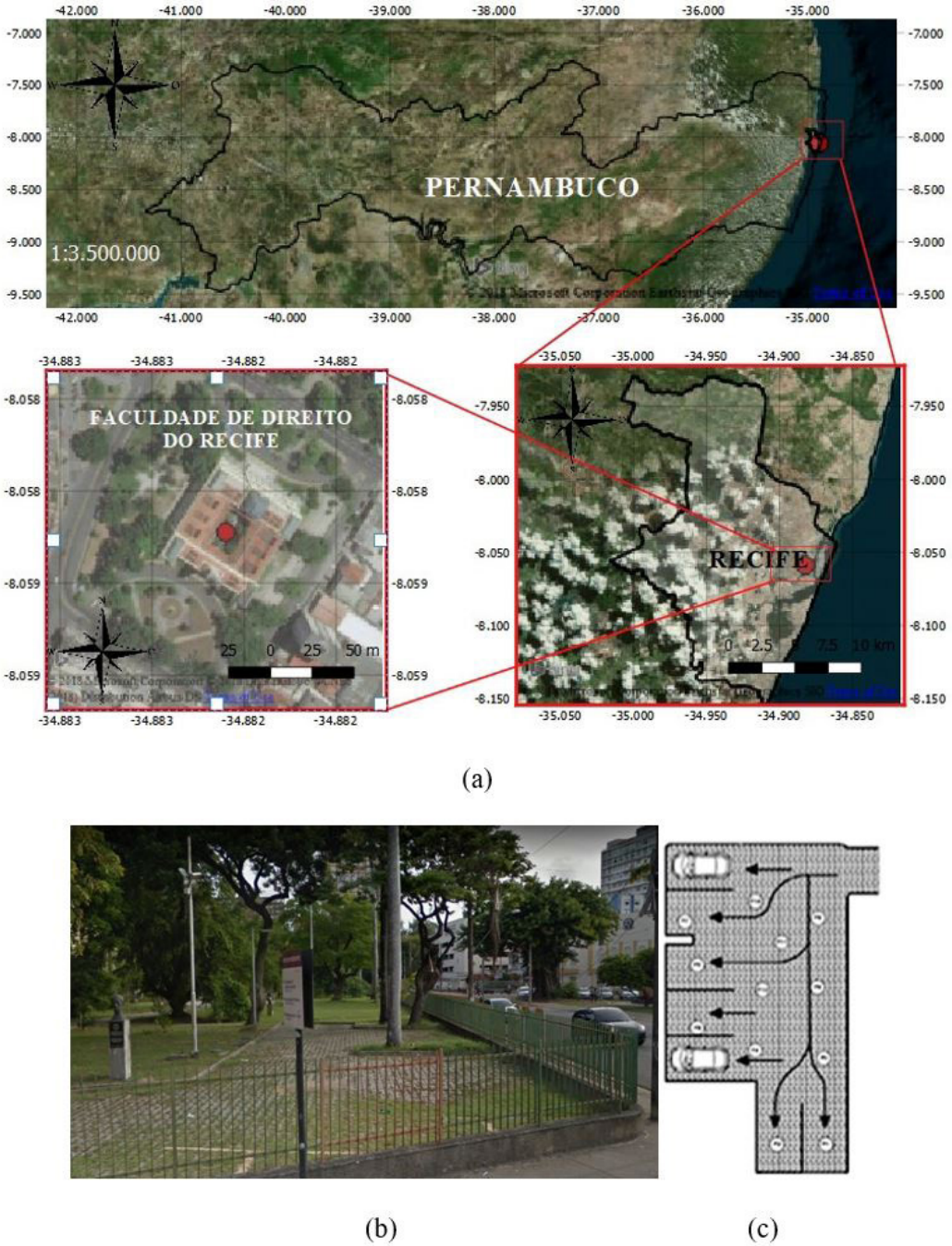

Figure 1. Localization of experimental study. (a) Satellite picture of the microregion of city of Recife-Brazil where field experiment was conducted; (b) Photo of the site; (c) Sketch of the study area.

Infiltration experiments

In order to verify the hydraulic and hydrological behavior of the PP, 12 points were chosen to perform the infiltration tests. The infiltration tests were carried out following the Beerkan methodology (until the time required for the infiltration of each water volume reaches steady state (permanent regime) (Mubarak et al., 2010; Coutinho et al., 2016). At each point the soil was sampled to determine the initial soil moisture condition ($cm^3.cm^{-3}$). After infiltrating the last applied volume, samples were taken to determine the final moisture ($cm^3.cm^{-3}$), particle size distribution and apparent density of the soil ($g.cm^{-3}$) in the 12 points. In the Figure 4c is presented the schematic location of the points for experimental tests in the field, the black narrows indicate the car direction flow in the parking lot.

Estimation of the soil hydraulic properties

The characterization of the hydraulic properties of PP was carried out using the BEST method (Beerkan Estimation of Soil Transfer Parameters through Infiltration Experiments) (Lassabatère et al., 2006; Souza et al., 2008). This method has

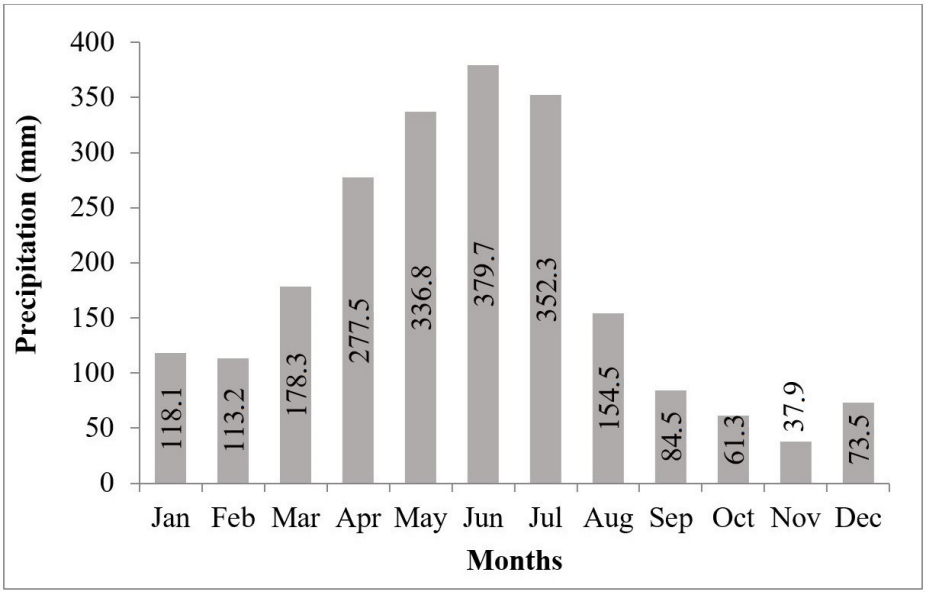

Figure 2. Average monthly and total annual rainfall of city of Recife-Brazil between the years 2010 to 2017 in the Várzea Station. Adapted from Agência Pernambucana de Águas e Clima (2018).

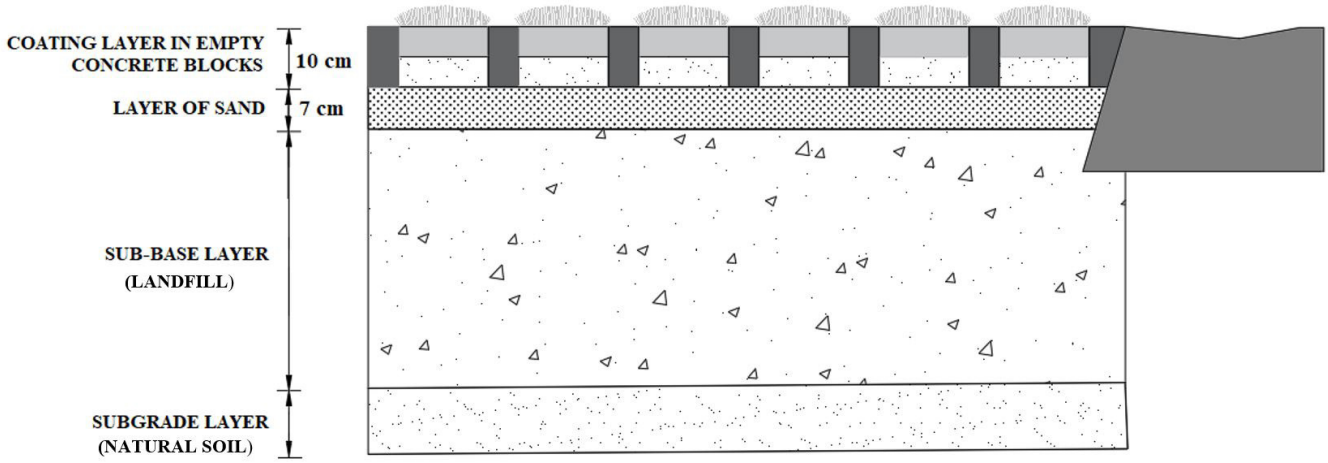

Figure 3. Permeable Pavement structure.

the advantage of providing a complete characterization of the hydraulic conductivity curve and the soil water retention curve. The parameters of the hydraulic conductivity curve of the soil $K(\theta)$ were described by the Brooks & Corey (1964) model (Equation 1). The parameters of the water retention curve $\theta(h)$ were described by the Van Genuchten (1980) with Burdine (1953) method (Equation 2).

$$\frac{K(\theta)}{K_s} = \left(\frac{\theta - \theta_r}{\theta_s - \theta_r}\right)^{\eta} \quad (1)$$

where $\eta = \frac{2}{m \cdot n} + 2 + p$

$$\frac{\theta - \theta_r}{\theta_s - \theta_r} = \left[1 + \left(\frac{h}{h_g}\right)^n\right]^{-m} \quad (2)$$

where $m = 1 - \frac{2}{n}$

The θ is the volumetric humidity ($L^3.L^{-3}$); θ_r and θ_s the residual and saturated volumetric humidity ($L^3.L^{-3}$), respectively; h the matric potential (L); h_g (L) a scale value of h considered the potential for air intake; m and n are shape parameters; K_s the saturated hydraulic conductivity of the soil ($L.T^{-1}$) and η the shape parameter for the hydraulic conductivity curve. The parameter p is a tortuosity, that depends on the capillary model, that is, zero (Childs & Collis-George, 1950), 0.5 (Mualem, 1976), 1 (Burdine, 1953), or 1.33 (Millington & Quirk, 1961).

To estimate all hydraulic parameters, the BEST method requires two sets of data: (1) the particle size distribution and the apparent density of the soil and (2) the infiltration accumulated throughout the infiltration experiment and the initial and final

(a) (b)

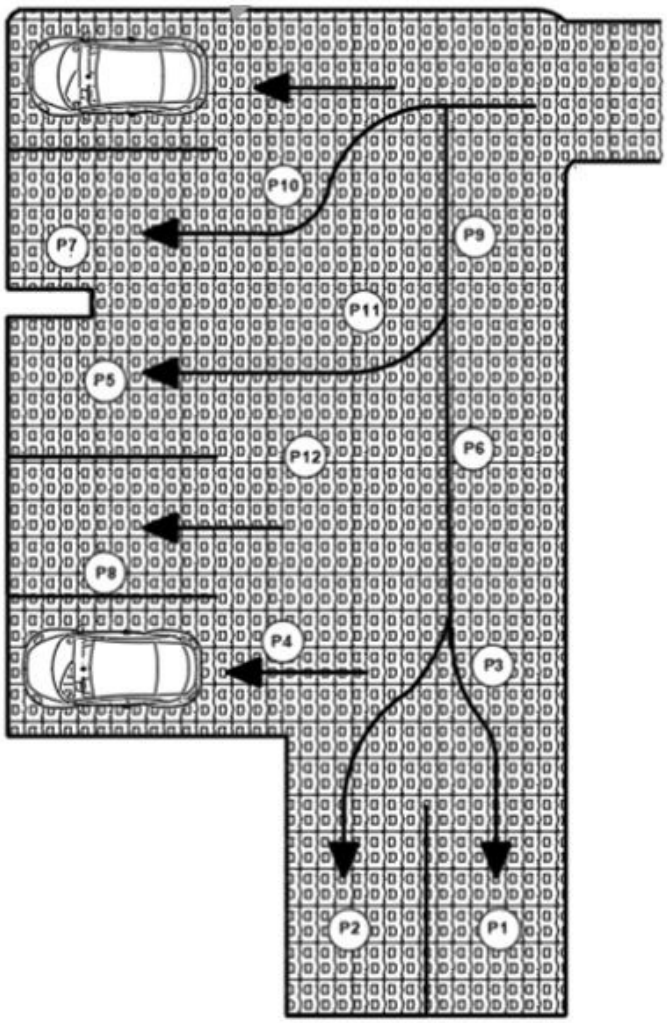

(c)

Figure 4. (a) and (b) Simple infiltration ring with a diameter of 100 cm positioned on the PP and properly sealed with bentonite for the infiltration experiments; (c) Idealized scheme of the locations of the 12 points of the experimental study.

humidity. In the BEST θ_r is considered zero. The humidity in saturation θ_s it is derived from the value of the apparent density of the soil assuming that it is equal to porosity. The shape parameter n was estimated from a pedotransfer function developed from the particle size distribution of the smaller fractions than 2 mm (Lassabatère et al., 2006). The scale parameters K_s and h_g are derived from the analysis of accumulated infiltration.

The shape parameters are linked to the texture and have similar shape between the particle size distribution $F(D)$ and $\theta(h)$. Haverkamp & Parlange (1986) presented the Equation 3 to express $F(D)$.

$$F(D)=\left[1+\left(\frac{D_g}{D}\right)^n\right]^{-m} \tag{3}$$

where

$$m=1-\frac{2}{n}$$

Being D the particle diameter (mm); Dg the particle size scale parameter (mm); m and n the shape parameters of the particle size distribution curve.

In turn, the normalization parameters depend on the soil structure. The parameters h_g and K_s are obtained by minimizing $I(S, K_s)$, that is, of the squares of the differences between the infiltrated water observed and calculated. The infiltrated water depth is calculated using the equation proposed by Haverkamp et al. (1994), valid for short and medium times (Equation 4).

$$I(S,K_s)=\sum_{i=1}^{Nobs}\left(I_i-\left(S.\sqrt{t_i}+a.S^2.t_i+b_2.K_s.t_i\right)\right)^2 \tag{4}$$

where a and b_2 are obtained by Brooks & Corey (1964):

$$a=\frac{\gamma}{r.\Delta\theta} \tag{5}$$

$$b_2=\left(\frac{\theta_0}{\theta_s}\right)^{\eta}+\frac{2-\beta}{3}.\left(1-\left(\frac{\theta_0}{\theta_s}\right)^{\eta}\right) \tag{6}$$

where S is the sorptivity; r is the cylinder radius; γ and β are coefficients that are commonly set at 0.75 and 0.60 (Haverkamp et al., 1994). $\Delta\theta = \theta s - \theta_0$, which apply for most soils when $\theta_0 < 0.25\ \theta s$ (Smettem et al., 1994; Haverkamp et al., 1994).

To minimize $I(S, K_s)$ is used the algorithm of Levenberg-Marquardt, iteration technique used to find the minimum of a function expressed as the sum of squares of non-linear functions (Marquardt, 1963). The Levenberg-Marquardt method is the determination of the vertex of a parabola. The performance of the adjustments analyzed by the values that correspond to the mean square error. Obtained the values of θ_s and K_s, the scale parameter for water pressure is determined h_g, by Equation 7 (Lassabatère et al., 2006).

$$h_g=\frac{S^2}{c_p(\theta_s-\theta_0)\left[1-\left(\frac{\theta_0}{\theta_S}\right)^{\eta}\right]k_s} \tag{7}$$

Being c_p a parameter that depends only on the parameters n, m and η (Condappa et al., 2002; Haverkamp et al., 1998), determined in Equation 8.

$$c_p=\Gamma\left(1+\frac{1}{n}\right)\left[\Gamma\frac{\left(m\eta-\frac{1}{n}\right)}{\Gamma(m\eta)}+\frac{\Gamma\left(m\eta+m-\frac{1}{n}\right)}{\Gamma(m\eta+m)}\right] \tag{8}$$

Γ is the classic Gamma function, which is an extension of the factorial function to numbers. During the three-dimensional infiltration process the factors that can affect the flow of water into the soil, that are: the geometry of the water source, capillarity and gravity (Lassabatère et al., 2019). One of the ways to characterize these factors is from the capillary length scales (λ_c) (White & Sully, 1987) and the characteristic radius of the hydraulically active pores (λ_m) (Philip, 1987), determined by Equations 9 and 10, respectively:

$$\lambda_c=\frac{\delta S^3}{(\theta_s-\theta_0)K_s} \tag{9}$$

$$\lambda_m=\frac{\sigma}{\rho_a g\lambda_c} \tag{10}$$

Being σ the surface tension of the water (0.0719 $N.m^{-1}$); ρ_a the specific gravity of water (10^3 $Kg.m^{-3}$); g the gravity acceleration; δ a diffusivity shape parameter [$1/(2\leq\delta\leq\pi/4)$], which was considered 0.55 (White & Sully, 1987).

According Souza et al. (2008), the capillary length scale represents the relative importance of capillary forces in relation to gravity, when water is transmitted from a source through the soil, with initial humidity θ_0. The characteristic pore radius defines the average size of the pores that participate in the infiltration process subjected to applied pressure h; the larger the characteristic radius, λ_m, greater is the effect of gravity compared to that of capillarity.

The number of pores $C_{\lambda m}$ is estimated using the Poiseuille law for flow in a capillary tube (Equation 11).

$$C_{\lambda m}=\frac{8\mu K}{\rho_a g\pi\lambda_m^4} \tag{11}$$

μ is the dynamic viscosity of the water (0.00089 $kg\cdot m^{-1}\cdot s^{-1}$).

The degree of variability of parameters was analyzed based on the classification proposed by Warrick & Nielsen (1980), who suggest CV limits <12%, 12<CV <52% and CV> 52% for low, medium properties and high variability, respectively.

RESULTS

Soil texture and infiltration curves

The particle size distribution curves are shown in Figure 5. The classification of soil texture was determined according to the fractions of clay, silt and sand (United States Department of Agriculture, 1987) and can be viewed on the (Appendix A). As a result, soil samples were divided into three main texture: Loamy sand (9 samples) (Figure 5a); Sandy loam (2 samples) (Figure 5b) and sand (1 sample) (Figure 5c). There is a predominance of the sand fraction with percentages above 80% in the 12 samples analyzed.

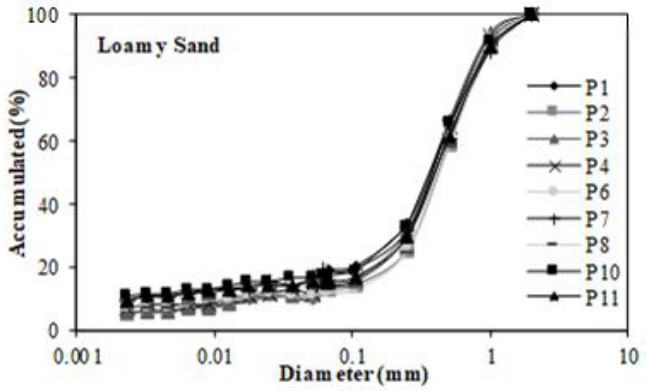

(a)

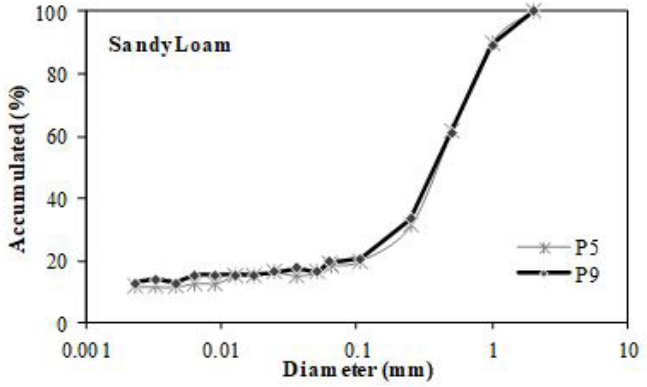

(b)

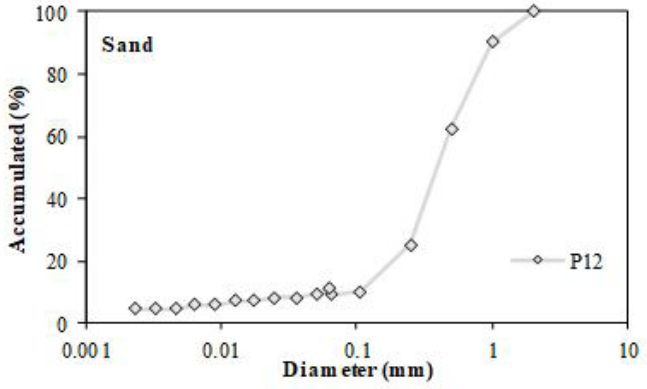

(c)

Figure 5. Particle Size Distribution. Loamy sand in (a); Sandy loam in (b) and; Sand in (c).

The lowest percentage of sand in the samples was 80.38% at Point 9 (Sandy Loam) and the highest 88.96% at Point 12 (sand).

The low percentage of clay and silt indicates a hydrological classification of the soil, according to the Soil Conservation Service in categories A or B (United States Department of Agriculture, 2009). Soils in this groups have low runoff potential and water is transmitted freely through the soil (United States Department of Agriculture, 2009).

- **Parameter $C_{\lambda m}$, λ_m and λ_c**

Table 1 shows the values of $C_{\lambda m}$, λ_m and λ_c, for the 12 sample points. The values of the capillary length scales (λ_c), characteristic radius of hydraulically active pores (λ_m) and the number of pores ($C_{\lambda m}$) varied from 784.85 (Point 11) to 82.73 mm (Point 6); 0.088592 (Point 6) to 0.009338 mm (Point 11); 9.02×10^{10} (Point 11) to 5.27×10^{6} pores/m^2 (Point 6), respectively. Point 7 was discarded, as it did not show numerical convergence with the Beerkan method, not meeting the criteria of the method.

Water infiltration experiments and hydraulic characterization

The Figure 6 presents the accumulated infiltration as a function of time for the 12 experiments. In the Loamy Sand (Figure 6a), the smallest blade infiltrated was 356.51 mm in 3.30 h and the highest of 891.27 mm in 2.07 h. In the Sandy Loam (Figure 6b) the smallest blade infiltrated was 509.30 mm in 2,43 h and the highest of 611.16 mm in 2.43 h. To sand (Figure 6c) the blade infiltrated was 534.76 mm in 2.03 h.

According to Figure 6, the curves show that there is a significant spatial variability in the infiltration behavior on the surface of the PP. Despite the variability, the response curves of Loamy Sand and Sandy Loam are in the same order of magnitude and resemble the curve of the sand. The different infiltration behaviors distributed in the PP can be attributed to the interference of other factors such as degree of compaction, dimension and connectivity between the pores (Lassabatère et al., 2010; Aiello et al., 2014), content of organic matter, in addition to the textural class (Coutinho et al., 2016).

Analyzing the average infiltration rates, it is noted that the average response is similar for all types of soil of the PP. The average infiltration rate was 4.56 mm·min^{-1}, the texture of Loamy Sand presented an average rate of 4.44 mm·min^{-1}, the Sandy Loam 5.03 mm·min^{-1} and the sand presented 4.24 mm·min^{-1}. It is important to highlight that the small number of samples does not allow to characterize the dispersion in detail for textural classes Sandy Loam and Sand. The observed differences in the infiltration rates considering all the experiments also indicate

Table 1. Values of the capillary length scales (λ_c), characteristic radius of hydraulically active pores (λ_m) and the number of pores ($C_{\lambda m}$) of 12 sample points.

Points	[a]$C_{\lambda m}$ (pores/m^2)	[b]λ_m (mm)	[c]λ_c (mm)
1	2.27E+10	0.016185	452.847
2	5.62E+09	0.021204	345.657
3	3.20E+09	0.019363	378.5206
4	2.64E+09	0.022174	330.5273
5	6.42E+10	0.01081	678.0292
6	5.27E+06	0.088592	82.73048
8	4.68E+08	0.036689	199.7685
9	1.36E+10	0.012767	574.0949
10	5.69E+08	0.026914	272.3219
11	9.02E+10	0.009338	784.8517
12	2.54E+09	0.021097	347.4111

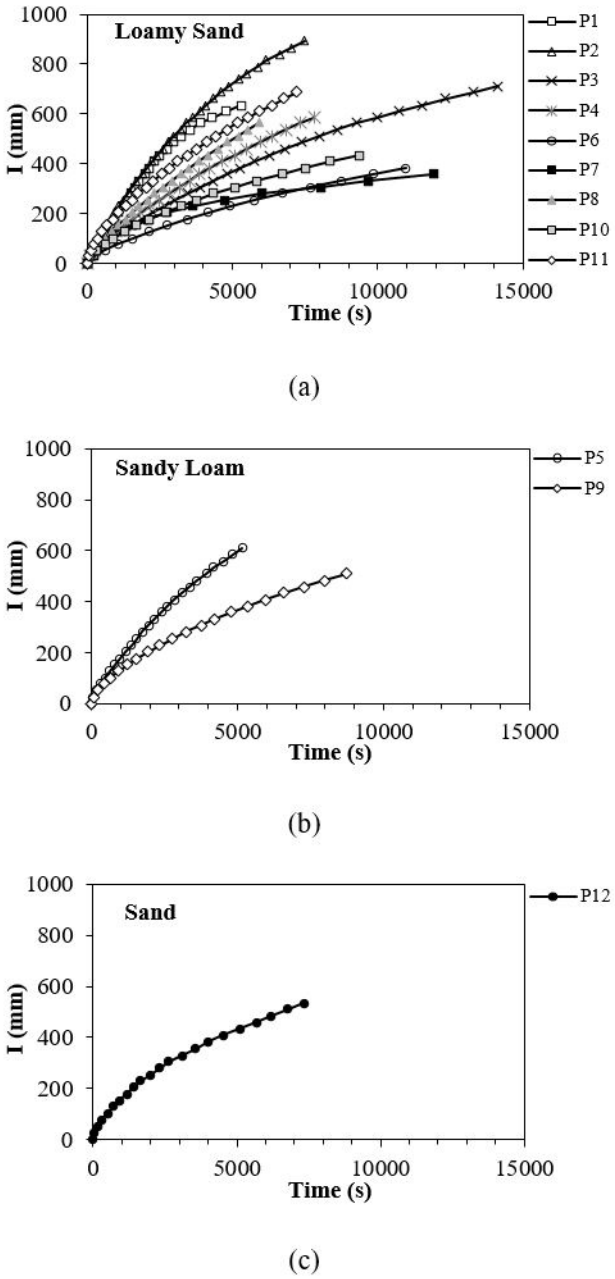

Figure 6. Accumulated Infiltrated Blade(mm) in function of time (s) of 12 PP infiltration experiments. Loamy sand in (a); Sandy loam in (b) and; Sand in (c).

moderate variability of the infiltration on the surface of the PP, as well as within the same type of texture. Based on the classification proposed by Warrick & Nielsen (1980), the statistical parameters of the infiltration rate in the permeable pavement indicated average variability, with a CV of 35.37% in the data with intermediates and coefficients of variation (12 < CV <52%)

In the same way, Coutinho et al. (2016) obtained an average infiltration rate of 14.5 mm·min^{-1} for a PP with interlocking concrete blocks and high spatial variability in the infiltration capacity through the Beerkan method. Jabur et al. (2015) obtained infiltration rate between 1.67 mm·min^{-1} and 2.84 mm·min^{-1} for a permeable pavement of interlocked concrete blocks. Bruno et al. (2013) obtained an infiltration rate of 1.4 mm·min^{-1} in an experimental plot of interlocked concrete blocks. Bean et al. (2007) obtained an infiltration rate of 0.84 mm.min^{-1} for permeable pavement applied to sidewalks and parking lots without routine maintenance and 1.44 mm.min^{-1} for permeable pavement applied to sidewalks and maintenance parking.

In general, the infiltration rates of all curves fall to a value that tends to the permanent regime. Only at Point 1 or Point 7 (Loamy Sand), the infiltration rate starts from 6.67 mm.min-1 and increases up to 13.3 mm.min^{-1} According to the infiltration theory, this is a lagged process, so that the appearance of phenomena such as the acceleration of the infiltration rate, is reported in the literature as hydrophobicity (Bastos et al., 2005; Maia et al., 2010; Vogelmann, 2014). According Vogelmann (2014), this is due to changes in the contact angle between water and the solid phase. By covering the soil particles by organic hydrophobic substances (such as leaves and roots) that cause water repellency.

It can be seen that P9, P10, P6 and P3 presented the lowest actual infiltration rates, due to the intense and constant traffic of the vehicles in the places of access to the spaces and maneuver, which cause the compaction. That is, reduction of the void volume of the soil (reduce its porosity) that generates the increase of the impermeability index (Bean et al., 2004). And the presence of leafy trees that protect the soil from direct irradiation, which also have scattered roots with a large radius of influence on the soil (which may be observed in the Figure 1b), can also interfere with water infiltration into the pavement (Fini et al., 2016). According to the tested points, the average of the infiltration rate was 355 mm·h^{-1}, being the lowest found in P6 (149.02 mm·h^{-1}) and the highest for P1 (527.80 mm·h^{-1}).

In addition, in this work it was not possible to make a correlation between the decrease of the infiltration rate with the classification by the textural triangle, since soils with the same textural classification presented very different values. This difference in hydraulic properties may be caused by factors that directly interfere with hydraulic conductivity how soil texture and structure, pore size and connectivity (Rahmati et al., 2018).

BEST results

Shape parameters

The BEST algorithm estimates the shape parameters based on the size of the particles and calculates the infiltration capacity by adjusting the infiltration rate as a function of time, using the theoretical model of Haverkamp et al. (1994). As a prerequisite for the application of the BEST method, the infiltration curve has to be described satisfactorily by the model, both in the permanent and in the transient regime (Lassabatère et al., 2010; Di Prima et al., 2016). Most of the accumulated infiltration curves from this work were well adjusted by the BEST method.

In Figure 7 box-plot graphs of shape parameters are presented, separated by soil type. The values of *n* varied between 2.23 e 2.24 to the soil Sandy Loam, 2.23 a 2.37 to the Loamy Sand and 2.43 to the sand. It is important to highlight that the values of *n* are higher on coarse soils than on thin soils. The *n* values are reported to the soil Loamy Sand between 2.42 and 2.56, Santos et al.

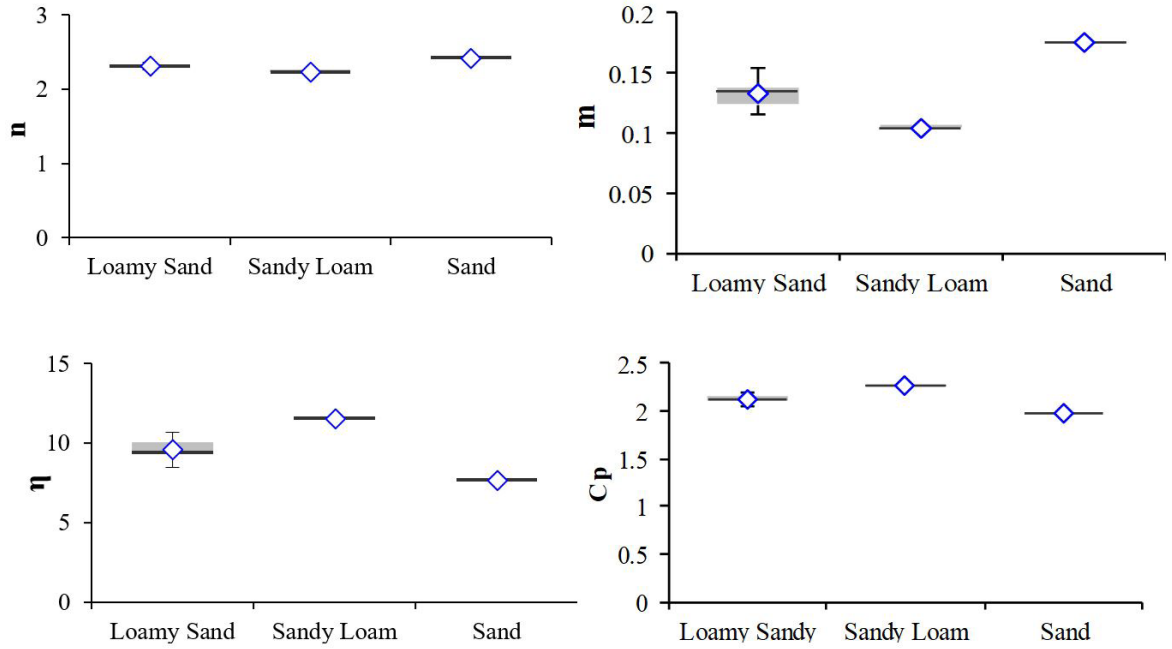

Figure 7. Box-plots of m, n, η e c_p parameters. The average of the parameters was calculated between the BEST Slope and BEST Intercept methods.

(2012), and 2.31, Souza et al., 2008. Studies conducted with sand soil report values of n between 2.54 e 2.88 (Coutinho et al., 2016; Santos et al., 2012; Souza et al., 2008). Santos et al. (2012) obtained n of 2.19 and 2.42, to a Sandy Loam soil, and Souza et al. (2008) obtained n between 2.13 and 2.16 for that same type of soil.

Small changes in the n values provide substantial differences in η. The values of η varied between 7.67 to 11.63 in this study considering all the soils studied. Some works with predominantly sandy soils such as Souza et al. (2008) obtained values η between 6.70 and 18.16, Silva et al. (2009) between 6.23 and 8.09 and Santos et al. (2012) between 1.34 and 7.83. Comparatively, the values of m, n, η and c_p obtained by Souza et al. (2008), Silva et al. (2009), Santos et al. (2012) and Coutinho et al. (2016), for the same textural classes they are compatible with those obtained in this study.

The shape parameters in general depend on the type of soil. The parameter values n and m for coarser soils (predominantly sandy soils) they are usually high. This can illustrate the piston effect of the conductivity and water retention curves on coarse materials. The piston effect is related to the condition of an abrupt increase in hydraulic conductivity and soil moisture in potential matrixes close to zero. In contrast, the shape parameter values for thin materials are lower and result in smoother retention and conductivity curves (Coutinho et al., 2016). The values presented in this work were higher in soils that have higher sand content and inversely the values of η and c_p were smaller for the same points.

Scale parameters

Primarily, normalization parameters do not depend on the type of soil. Among the normalization parameters adjusted by BEST, the average pore length (h_g) it depends directly on the structure of the soil. Saturated hydraulic conductivity (K_s) is the parameter that indicates how easily a fluid is transported through the soil. Sorptivity (S) corresponds to the capacity of the soil to absorb water by capillarity in the absence of gravitational effects (Borges et al., 1999). In Figure 8 box-plot graphs of normalization parameters (h_g, K_s and S) are shown adjusted by BEST Slope and Intercept separated by soil type.

The average pore length (h_g) varied between -229.952 to -365.303 mm in the BEST Intercept and -268.475 to -803.886 mm in the BEST Slope. Considering all the experiments it is possible to highlight that the values of h_g in BEST Slope they were higher than the Intercept values. Analyzing the values of h_g to the Loamy Sand (n=9), by BEST Slope the values of h_g varied between -268.475 and -778.441 mm and BEST Intercept varied between -229.952 and -365.303 mm. In the same way for the soil Sandy Loam (n=2) the h_g values by BEST Slope varied between -481.775 to -781.085 mm and by BEST Intercept varied between -337.601 to -357.445 mm. The sandy soil (n=1) presented the highest value of h_g considering the two methods and all studied soils, h_g = -803.886 mm by Slope.

The Ks values determined by the BEST Intercept are higher than the values of the BEST Slope. The Ks values of Loamy Sand soil by the BEST Intercept varied between 0.0153 and 0.0706 mm.s^{-1}, by BEST Slope 0.008 and 0.064 mm.s^{-1}. In the Sandy Loam soil, the BEST Intercept estimated Ks between 0.0323 and 0.01057 mm.s^{-1} and BEST Slope estimated the Ks values between 0.0434 and 0.0293 mm.s^{-1}. The Ks values estimated by the BEST Intercept were also higher than the values of Ks estimated by BEST Slope for Sand soil. These results for Loamy Sand and Sandy Loam are in accordance with several studies in the literature (Souza et al., 2008; Di Prima et al., 2017; Sousa et al., 2019; Lassabatère et al., 2019).

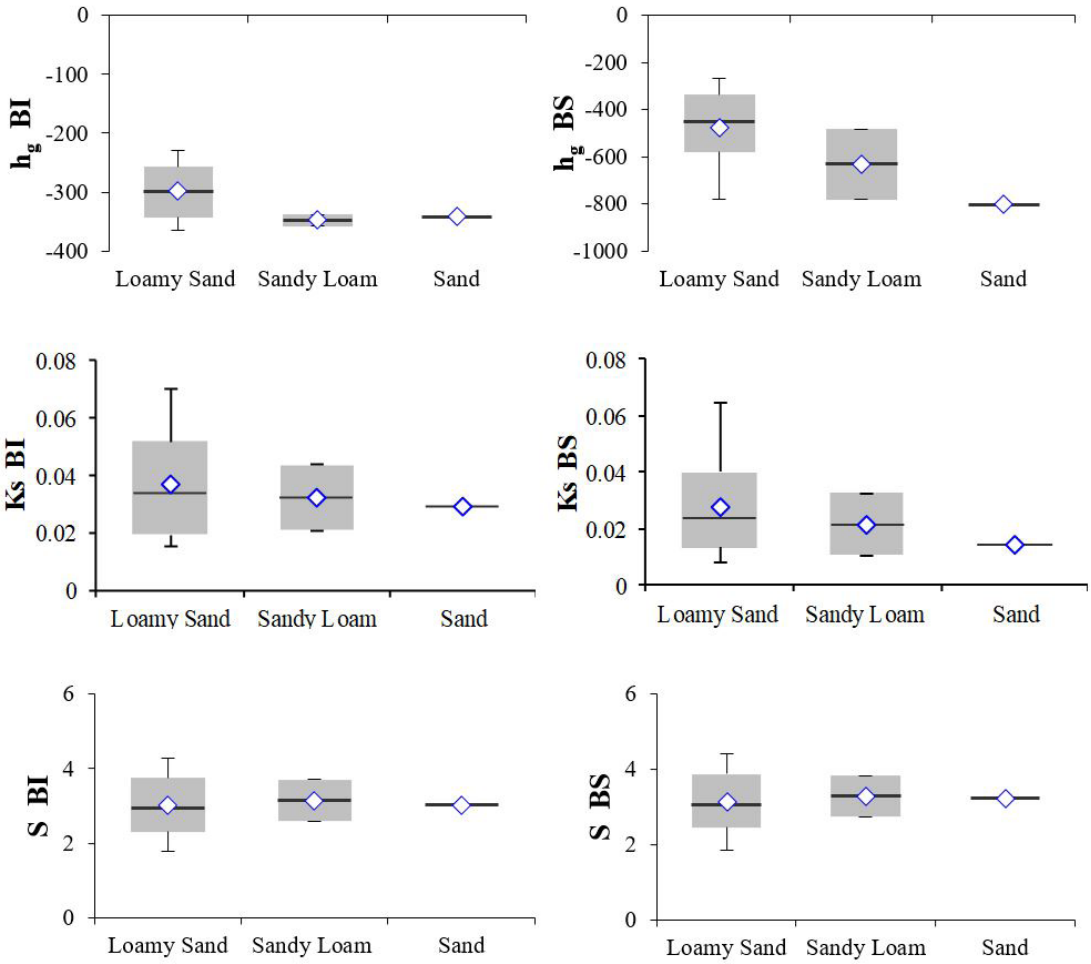

Figure 8. Box-plots of normalization parameters, K_s in mm.s^{-1}, h_g in mm and S in mm.s$^{0.5}$ classified by soil type for BEST Slope (BS), BEST Intercept (BI).

The Sorptivity values estimated by BEST slope and intercept were similar, with BEST slope values slightly higher. The greatest value of Sorptivity was 4.416 mm.s$^{-0.5}$ of Loamy Sand soil by Slope and the lowest value was 1.7984 mm.s$^{-0.5}$ to Loamy Sand soil by Intercept. For some cases where the portion of Sorptivity is very large, BEST Slope can estimate null or negative values of saturated hydraulic conductivity, in this case BEST Intercept corrects the error (Yilmaz et al., 2010).

Analyzing the results according to the texture, it is expected that the highest values of K_s and S they should have occurred on Sand-type soil. However, the extreme values occurred within the texture Loamy Sand. This is due to the K_s and S be parameters that depend on factors other than texture, such as the apparent density of the soil and connectivity between the hydraulically active pores (Castellini et al., 2019). These results highlight the importance of the soil structure for its hydraulic behavior (Lassabatère et al., 2019). In general, the saturated hydraulic conductivity is of the same order of magnitude for all types of soil in this study. There were significant differences between the two BEST methods in estimating the scale parameter for water pressure. Noting that there are only two Sandy Loam soil samples and a sample of sand the focus should be placed on the most frequent type of soil (Loamy Sand).

Retention and hydraulic conductivity curves

Defined the shape parameters (m or n and η) and scale (θ_s, K_s and h_g), retention curves were obtained $\theta(h)$ and hydraulic conductivity $K(\theta)$. The points of origin of each curve (θ_s) were set in 0.46792 m^3.m^{-3}, considering the same volumetric humidity for all experiments. According Di Prima et al. (2016), the estimates for the scale parameters depend on the BEST methods chosen. However, in this study, the use of the Slope and Intercept methods led to results comparable with similar trends in most parameters. Given the dependence of the method, it was decided to average the values of the scale parameters in both methods. Table 2 shows the averages of hydraulic parameters by type of soil. Based on these values, the hydraulic conductivity curve and the water retention curve were plotted (Figure 9).

In relation to hydraulic conductivity, the most sandy soil presented less hydraulic conductivity in saturation. Regarding the soil water retention curve $\theta(h)$, it was observed that all cases presented very similar curves. The higher the percentage of sand, the lower the water retention capacity in the soil. In general, soils with a high percentage of sand (as in the case of the study) have many hydraulically active pores. Fine Soils or clayey soils presents a

Table 2. BEST derived hydraulic parameters depending on soil types (average).

Texture	h_g (mm)	K_s (mm/h)	n	m	η	c_p	S (mm/s$^{0.5}$)
Loamy Sand	-387.08	115.7288	2.30875	0.13375	9.5675	2.13	3.0875
Sandy Loam	-489.48	96.42	2.235	0.105	11.56	2.255	3.2175
Sand	-572.79	78.525	2.43	0.18	7.67	1.98	3.135

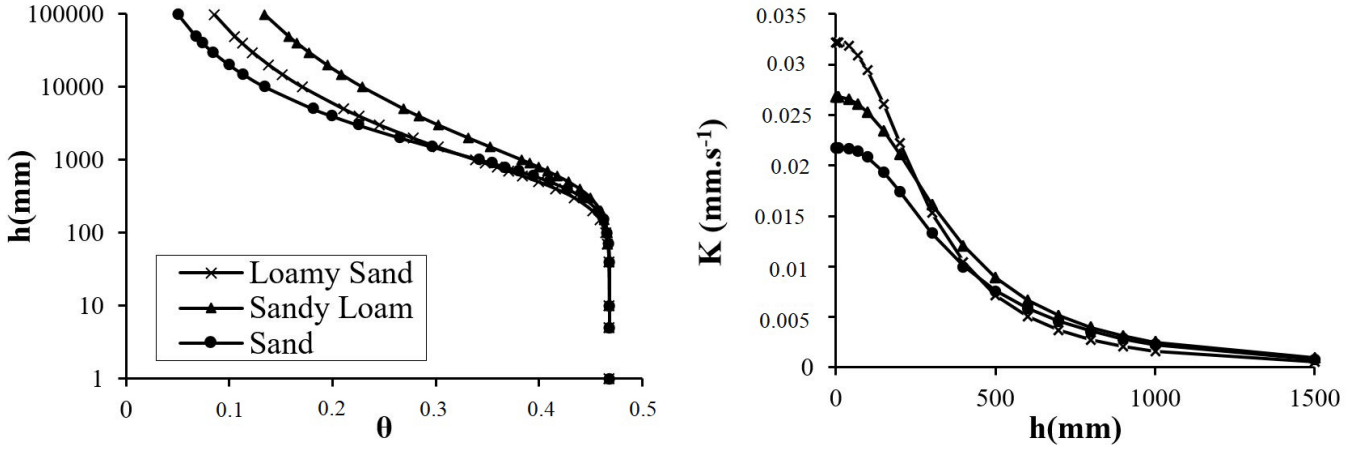

Figure 9. Hydraulic conductivity and water retention curves for the three types of soil.

greater proximity between the particles, results in higher adsorption and capillarity effects and most capacity of retention of water. The saturated hydraulic conductivity curves *Ks* contribute to a better understanding of hydraulic behavior at the points tested. For greater volumetric water content *(θ)*, the *K(θ)* values tend to increase in soils with a higher percentage of Sand.

CONCLUSIONS

The present study evaluated the infiltration capacity of a permeable pavement (PP) of hollow concrete blocks. The hydraulic characterization and the infiltration capacity were analyzed in real scale, using a simple ring infiltrometer of 100 cm in diameter through the Beerkan method.

In this experimental work, 12 points of a permeable pavement consisting of concrete blocks filled with compacted soil were evaluated. From the results obtained, the following conclusions are presented:

The dispersion of the observed infiltration rate set of values demonstrated intermediate variability of pavement infiltration capacity. This variance may be due to the degree of compaction that interferes with the arrangement of the particles and pore connectivity due to the pavement usage conditions. Besides, the presence of organic matter, boulders, and other contaminants in the floor void filling soil, as well as in the lower layers, modify the behavior and the rate of water transfer into the soil (i.e. hydrophobicity phenomenon, observed in P1).

The Beerkan method produced, quickly, simply and at a low cost, an important set of data that helped evaluating and characterize the capacity of PP of hollow blocks as a compensatory technique. The BEST algorithm obtained acceptable values for S and *Ks*, in 11 of 12 analyzed points, besides providing precise adjustments of the accumulated infiltrations.

The results obtained in this study through the estimation of the hydraulic parameters can demonstrate the hydraulic efficiency of the PP of hollow blocks for the Decrease of the effective precipitation through the use of simulation models that allow evaluating the dynamics of the water in these structures. Also, the monitoring of the hydraulic behavior of permeable pavements at field scale using infiltration tests allows the knowledge of the hydrological performance of these structures, allowing them to be used and integrated with urban environments knowing their limitations.

ACKNOWLEDGEMENTS

This work was carried out as part of the author's PhD research, at the Federal University of Pernambuco, in the Postgraduate Program in Civil Engineering, and with support of the project "Transfer of Water and Mixtures of Reactive Pollutants in Anthropized Soils" (CNPq process n°. 436875/2018-7). Part of the tests were carried out with the support of the Nuclear Energy Department-UFPE and Center for Legal Sciences -UFPE.

REFERENCES

Agência Pernambucana de Águas e Clima – APAC. (2018). *Monitoramento pluviométrico.* Retrieved in 2018, February 18, from http://www.apac.pe.gov.br/meteorologia/monitoramentopluvio.php?posto_id=0

Agostinho, M. S. P., & Poleto, C. (2012). Sistemas sustentáveis de drenagem urbana: dispositivos. *Holos Environment*, *12*(2), 121-131. http://dx.doi.org/10.14295/holos.v12i2.3054.

Aiello, R., Bagarello, V., Barbagallo, S., Consoli, S., Di Prima, S., Giordano, G., & Iovino, M. (2014). An assessment of the Beerkan method for determining the hydraulic properties of a sandy loam soil. *Geoderma*, *235*, 300-307. http://dx.doi.org/10.1016/j.geoderma.2014.07.024.

American Society for Testing and Materials – ASTM. (2009). *C1701: standard test method for infiltration rate of in place pervious concrete*. Pennsylvania: ASTM.

Associação Brasileira de Normas Técnicas – ABNT. (2016). *NBR 7181: análise granulométrica*. Rio de Janeiro: ABNT.

Bastos, R. S., Mendonça, E. S., Alvarez V, V. H., & Corrêa, M. M. (2005). Soil aggregate formation and stabilization as influenced by organic compounds with different hydrophobic characteristics. *Revista Brasileira de Ciência do Solo*, *29*(1), 11-20. http://dx.doi.org/10.1590/S0100-06832005000100002.

Bean, E. Z., Hunt, W. F., & Bidelspach, D. A. (2007). Field survey of permeable pavement surface infiltration rates. *Journal of Irrigation and Drainage Engineering*, *133*(3), 249-255. http://dx.doi.org/10.1061/(ASCE)0733-9437(2007)133:3(249).

Bean, E. Z., Hunt, W. F., & Bidelspach, D. A. (2004). Study on the surface infiltration rate of permeable pavements. In G. Sehlke, D. F. Hayes & D. K. Stevens (Eds.), *Critical transitions in water and environmental resources management* (pp. 1-10). Reston: American Society of Civil Engineers.

Benini, S. M. (2015). *Infraestrutura verde como prática sustentável para subsidiar a elaboração de planos de drenagem urbana: estudo de caso da cidade de Tupã/SP* (Tese de doutorado). Faculdade de Ciências e Tecnologia de Presidente Prudente, Universidade Estadual Paulista "Júlio de Mesquita Filho", Presidente Prudente.

Borges, E., Antonino, A. C. D., Dall'Olio, A., Audry, P., & Carneiro, C. J. G. (1999). Determinação da condutividade hidráulica e da sorvidade de um solo não saturado utilizandose permeâmetro a disco. *Pesquisa Agropecuária Brasileira*, *34*(11), 2083-2089. http://dx.doi.org/10.1590/S0100-204X1999001100015.

Brooks, R. H., & Corey, A. T. (1964). *Hydraulic properties of porous media* (p. 27, Hydrology Paper, No. 3). Fort Collins: Colorado State University.

Bruno, L. O., Amorim, R. S. S., & Silveira, A. (2013). Estudo da redução do escoamento superficial direto em superfícies permeáveis. *Revista Brasileira de Recursos Hídricos*, *18*(2), 237-247. http://dx.doi.org/10.21168/rbrh.v18n2.p237-247.

Burdine, N. T. (1953). Relative permeability calculations from pore-size distribution data. *Journal of Petroleum Technology*, *5*(3), 71-78. http://dx.doi.org/10.2118/225-G.

Castellini, M., Stellacci, A. M., Tomaiuolo, M., & Barca, E. (2019). Spatial variability of soil physical and hydraulic properties in a durum wheat field: an assessment by the BEST-procedure. *Water*, *11*(7), 1434. http://dx.doi.org/10.3390/w11071434.

Childs, E. C., & Collis-George, G. N. (1950). The permeability of porous materials. *Proceeding of the Royal Society of London Series A*, *201*, 392-405.

Condappa, D., Soria Ugalde, J. M., Angulo-Jaramillo, R., & Haverkamp, R. (2002). *Méthode Beerkan: caractérisation des proprieties hydrodynamiques des sols non saturés: rapport interne Hydrologie de la Zone Non Saturés – LTHE* (p. 82). Grenoble: Université de Grenoble.

Coutinho, A. P. (2011). *Pavimento permeável como tecnica compensatória na drenagem urbana da cidade do Recife* (Dissertação de mestrado). Programa de Pós-graduação em Engenharia Civil, Universidade Federal de Pernambuco, Recife.

Coutinho, A. P., Lassabatere, L., Montenegro, S., Antonino, A. C. D., Jaramillo, R. A., & Cabral, J. J. S. P. (2016). Hydraulic characterization and hydrological behavior of a pilot permeable pavement in an urban centre, Brazil. *Hydrological Processes*, *30*, 4242-4254.

Coutinho, A. P., Ribas, L. V., Leite, L. L. L., Antonino, A. C. D., Cabral, J., Montenegro, S. M. G. L., & Melo, T. A. T. (2013). Determinação de equações de chuvas intensas para municípios das mesorregiões do estado de Pernambuco através do método de Bell. In *Anais do XX Simpósio Brasileiro de Recursos Hídricos*. Porto Alegre: ABRH.

Di Prima, S., Bagarello, V., Lassabatere, L., Angulo-Jaramillo, R., Bautista, I., Burguet, M., Cerdà, A., Iovino, M., & Prosdocimi, M. (2017). Comparing Beerkan infiltration tests with rainfall simulation experiments for hydraulic characterization of a sandy-loam soil. *Hydrological Processes*, *31*(20), 3520-3532. http://dx.doi.org/10.1002/hyp.11273.

Di Prima, S., Lassabatère, L., Bagarello, V., Iovino, M., & Angulo Jaramillo, R. (2016). Testing a new automated single ring infiltrometer for Beerkan infiltration experiments. *Geoderma*, *262*, 20-34. http://dx.doi.org/10.1016/j.geoderma.2015.08.006.

Empresa Brasileira de Pesquisa Agropecuária – EMBRAPA. Centro Nacional de Pesquisa de Solos. (1999). *Sistema brasileiro de classificação de solos*. Brasília: Embrapa Solos.

Fini, A., Frangi, P., Robbiani, E., & Ferrini, F. (2016). *Pervious vs. impervious pavements for sidewalks: effects on soil characteristics and physiology of two establishing urban tree species*. Atlanta: ISA.

Hager, J., Hu, G., Hewage, K., & Sadiq, R. (2019). Performance of low-impact development best management practices: a critical review. *Environmental Reviews*, *27*(1), 17-42. http://dx.doi.org/10.1139/er-2018-0048.

Haverkamp, R., & Parlange, J. Y. (1986). Predicting the water retention curve from particle size distribution: I Sandy soils without organic matter. *Soil Science*, *142*(6), 325-335. http://dx.doi.org/10.1097/00010694-198612000-00001.

Haverkamp, R., Parlange, J. Y., Cuenca, R., Ross, P. J., & Steenhuis, T. S. (1998). Scaling of the Richards equation and its application to watershed modeling. In G. Sposito (Ed.), *Scale dependence and scale invariance in hydrology* (pp. 190-223). Cambridge: Cambridge University Press. http://dx.doi.org/10.1017/CBO9780511551864.008.

Haverkamp, R., Ross, P. J., Smettem, K. R. J., & Parlange, J. Y. (1994). Three dimensional analysis of infiltration from the disc infiltrometer. 2. Physically based infiltration equation. *Water Resources Research*, *30*(11), 2931-2935. http://dx.doi.org/10.1029/94WR01788.

Jabur, A. S., Dornelles, F., Silveira, A. L. L., Goldenfum, J. A., Okawa, C. M. P., & Gasparini, R. R. (2015). Determinação da capacidade de infiltração de pavimentos permeáveis. *Revista Brasileira de Recursos Hídricos*, *20*(4), 937-945. http://dx.doi.org/10.21168/rbrh.v20n4.p937-945.

Lassabatère, L., Angulo-Jaramillo, R., Goutaland, D., Letellier, L., Gaudet, J. P., Winiarski, T., & Delolme, C. (2010). Effect of the settlement of sediments on water infiltration in two urban infiltration basins. *Geoderma*, *156*(3-4), 316-325. http://dx.doi.org/10.1016/j.geoderma.2010.02.031.

Lassabatère, L., Angulo-Jaramillo, R., Soria Ugalde, J. M., Cuenca, R., Braud, I., & Haverkamp, R. (2006). Beerkan estimation of soil transfer parameters through infiltration experiments - BEST. *Soil Science Society of America Journal*, *70*(2), 521-532. http://dx.doi.org/10.2136/sssaj2005.0026.

Lassabatère, L., Di Prima, S., Angulo-Jaramillo, R., Keesstra, S., & Salesa, D. (2019). Beerkan multi-runs for characterizing water infiltration and spatial variability of soil hydraulic properties across scales. *Hydrological Sciences Journal*, *64*(2), 165-178. http://dx.doi.org/10.1080/02626667.2018.1560448.

Li, C., Peng, C., Chiang, P. C., Cai, Y., Wang, X., & Yang, Z. (2019). Mechanisms and applications of green infrastructure practices for stormwater control: a review. *Journal of Hydrology*, *568*, 626-637. http://dx.doi.org/10.1016/j.jhydrol.2018.10.074.

Liu, J., Yan, H., Liao, Z., Zhang, K., Schmidt, A. R., & Tao, T. (2019). Laboratory analysis on the surface runoff pollution reduction performance of permeable pavements. *The Science of the Total Environment*, *691*, 1-8. PMid:31306873. http://dx.doi.org/10.1016/j.scitotenv.2019.07.028.

Maia, C. M. B. F., Fukamachi, C. R. B., Cambronero, Y. C., Dedecek, R. A., Mangrich, A. S., Narimoto, K. M., Milori, D. M. B. P., & Simões, M. L. (2010). Hidrofobicidade em Neossolo litólico sob plantação de Pinus taeda. *Pesquisa Florestal Brasileira*, *30*(62), 93. http://dx.doi.org/10.4336/2010.pfb.30.62.93.

Marquardt, D. W. (1963). An algorithm for least squares estimation of nonlinear parameters. *SIAM Journal on Applied Mathematics*, *11*(2), 431-441. http://dx.doi.org/10.1137/0111030.

Maruyama, C. M., & Franco, M. A. R. (2016). Pavimentos permeáveis e infraestrutura verde. *Periódico Técnico e Científico Cidades Verdes*, *4*(9), 73-86.

Millington, R. J., & Quirk, J. P. (1961). Permeability of porous solids. *Transactions of the Faraday Society*, *57*, 1200-1207. http://dx.doi.org/10.1039/tf9615701200.

Mualem, Y. (1976). A new model for predicting the hydraulic conductivity of unsaturated porous media. *Water Resources Research*, *12*(3), 513-522. http://dx.doi.org/10.1029/WR012i003p00513.

Mubarak, I., Angulo-Jaramillo, R., Mailhol, J. C., Ruelle, P., Khaledian, M., & Vauclin, M. (2010). Spatial analysis of soil surface hydraulic properties: is infiltration method dependent? *Agricultural Water Management*, *97*(10), 1517-1526. http://dx.doi.org/10.1016/j.agwat.2010.05.005.

Nunes, D. M., Alvarez, M. G. L., Ohnuma Junior, A. A., & Silva, L. P. (2017). Aplicação de técnicas compensatórias no controle dos escoamentos superficiais: estudo de caso em loteamento residencial em Jacarepaguá, Rio de Janeiro. *Revista Internacional de Ciências*, *7*(1), 3-21. http://dx.doi.org/10.12957/ric.2017.21887.

Philip, J. R. (1987). The quasilinear analysis, the scattering analog, and other aspects of infiltration and seepage. In Y. S. Fok (Ed.), *Infiltration development and application* (pp. 1-27). Honolulu: Water Resources Research Center.

Rahmati, M., Weihermüller, L., Vanderborght, J., Pachepsky, Y. A., Mao, L., Sadeghi, S. H., & Toth, B. (2018). *Development and analysis of the Soil Water Infiltration Global database*. Brasília: EMBRAPA.

Richards, L. A. (1931). Capillary conduction of liquids in porous mediums. *Physics*, *1*(5), 328-333. http://dx.doi.org/10.1063/1.1745010.

Santos, C. A. G., Silva, J. F. C. B. C., & Silva, R. (2012). Caracterização hidrodinâmica dos solos da bacia experimental do Riacho Guaíra utilizando o método Beerkan. *Revista Brasileira de Recursos Hídricos*, *17*(4), 149-160. http://dx.doi.org/10.21168/rbrh.v17n4.p149-160.

Silva, J. F. C. B. C., Rodrigues, A. C. L., Santos, C. A. G., & Silva, R. M. (2009). Caracterização hidrodinâmica de solos através da aplicação da metodologia Beerkan: estudo de caso na Bacia Experimental do Guaraíra - PB. In *Anais do XVIII Simpósio Brasileiro de Recursos Hídricos*. Porto Alegre: ABRH.

Smettem, K. R. J., Parlange, J. Y., Ross, P. J., & Haverkamp, R. (1994). Three-dimensional analysis of infiltration from the disc infiltrometer: 1. A capillary-based theory. *Water Resources Research*, *30*(11), 2925-2929. http://dx.doi.org/10.1029/94WR01787.

Sousa, N. M. D., Soares, W. D. A., Silva, S. R. D., & Nascimento, E. C. D. (2019). Contribution of public squares to the reduction of urban flooding risk. *Revista Ambiente & Água*, *14*(6), 1. http://dx.doi.org/10.4136/ambi-agua.2374.

Souza, C. F., Cruz, M. A. S., & Tucci, C. E. M. (2012). Desenvolvimento urbano de baixo impacto: planejamento e tecnologias verdes para a sustentabilidade das águas urbanas. *Revista Brasileira de Recursos Hídricos*, *17*(2), 9-18. http://dx.doi.org/10.21168/rbrh.v17n2.p9-18.

Souza, E. S., Antonino, A. C. D., Angulo-Jaramillo, R., & Netto, A. M. (2008). Caracterização hidrodinâmica de solos: aplicação do método Beerkan. *Revista Brasileira de Engenharia Agrícola e Ambiental*, *12*(2), 128-135. http://dx.doi.org/10.1590/S1415-43662008000200004.

Tucci, C. E. M. (2007). *Inundações urbanas*. Porto Alegre: ABRH.

United States Department of Agriculture – USDA. Soil Conservation Service. (1987). *Textural soil classification, soil mechanics level 1: module 3: study guide*. Washington: USDA.

United States Department of Agriculture – USDA. (1993). *Soil survey manual*. Washington: Natural Resources Conservation Service.

United States Department of Agriculture – USDA. (2009). Hydrologic soil groups. In United States Department of Agriculture – USDA, *Part 630: hydrology national engineering handbook*. Washington: USDA. Retrieved in 2018, February 18, from https://directives.sc.egov.usda.gov/viewerFS.aspx?hid=21422

Van Genuchten, M. T. H. (1980). A closed-form equation for predicting the hydraulic conductivity of unsaturated soils. *Soil Science Society of America Journal*, *44*(5), 892-898. http://dx.doi.org/10.2136/sssaj1980.03615995004400050002x.

Vogelmann, E. S. (2014). *Relações da matéria orgânica com a hidrofobicidade do solo* (Tese de doutorado). Universidade Federal de Santa Maria, Santa Maria.

Warrick, A. W., & Nielsen, D. R. (1980). Spatial variability of soil physical properties in the field. In D. Hillel (Ed.), *Applications of soil physics* (pp. 319-344). New York*:* Academic Press. http://dx.doi.org/10.1016/B978-0-12-348580-9.50018-3.

White, I., & Sully, M. J. (1987). Macroscopic and microscopic capillary length and times scales from field infiltration. *Water Resources Research*, *23*(8), 1514-1522. http://dx.doi.org/10.1029/WR023i008p01514.

Yilmaz, D., Lassabatere, L., Angulo-Jaramillo, R., Deneele, D., & Legret, M. (2010). Hydrodynamic characterization of basic oxygen furnace slag through an adapted BEST method. *Vadose Zone Journal*, *9*(1), 107-116. http://dx.doi.org/10.2136/vzj2009.0039.

Authors contributions

Marília Neves Marinho: Conceptualization; Methodology; Software; Validation; Formal analysis; Investigation; Data curation; Writing – original draft; Visualization.

Artur Paiva Coutinho: Conceptualization; Methodology; Software; Validation; Resources; Writing – review and editing; Supervision; Project administration; Funding acquisition.

Severino Martins dos Santos Neto: Conceptualization; Methodology; Writing – review and editing; Writing – original draft.

Cézar Augusto Casagrande: Investigation; Resources; Writing – original draft.

Guilherme Teotônio Leite Santos: Investigation; Data curation; Writing – original draft.

Arnaldo Manoel Pereira Carneiro: Writing – review and editing; Supervision; Project administration; Funding acquisition.

Appendix A. Supplementary Data.

Table 1A. Clay, Silt and Sand contents of 12 points of PP infiltration.

Sample	Clay(%)	Silt(%)	Sand(%)	Texture (USDA)
P1	5.86	10.00	84.14	Loamy Sand
P2	4.69	8.28	87.03	Loamy Sand
P3	5.86	9.14	85.00	Loamy Sand
P4	7.03	7.68	85.29	Loamy Sand
P5	11.72	7.54	80.73	Sandy Loam
P6	7.03	5.34	87.63	Loamy Sand
P7	9.38	10.11	80.51	Loamy Sand
P8	7.03	7.21	85.76	Loamy Sand
P9	12.89	6.72	80.38	Sandy Loam
P10	10.55	6.84	82.61	Loamy Sand
P11	9.38	5.80	84.82	Loamy Sand
P12	4.69	6.35	88.96	Sand